ELSEVIER

Biochimica et Biophysica Acta 1329 (1997) 159–168

BIOCHIMICA ET BIOPHYSICA ACTA
BBA

# The effect of phloretin on the hydration of egg phosphatidylcholine multilayers

Gordon L. Jendrasiak [a,*], Ralph L. Smith [a], Thomas J. McIntosh [b]

[a] *Department of Radiation Oncology, School of Medicine, East Carolina University, Leo Jenkins Cancer Center, Greenville, NC 27858-4354, USA*

[b] *Department of Cell Biology, Duke University Medical Center, Durham, NC 27710, USA*

Received 4 February 1997; revised 22 April 1997; accepted 28 April 1997

**Abstract**

The effect of phloretin on the hydration, structure and interactive properties of supported phospholipid bilayers has been studied by a combination of direct water adsorption measurements and X-ray diffraction. Adsorption isotherms show that over a wide range of relative vapor pressures (from 0 to approximately 1.0) the addition of 20 or 40 mol% phloretin significantly alters the amount of water adsorbed by egg phosphatidylcholine (EPC) multilayers. X-ray diffraction analysis shows that the incorporation of phloretin decreases the width of the EPC bilayer, thereby increasing the area per lipid molecule from approximately 64 $Å^2$ for EPC to about 78 $Å^2$ for EPC:Ph, 3:2, M:M. Phloretin also decreases the distance between apposing EPC bilayers, most likely because it causes a reduction in repulsive hydration/steric pressure between apposing bilayers. Because phloretin decreases the fluid layer between bilayers by a larger amount than it increases the area per EPC molecule, phloretin has the effect of decreasing the water volume in the multilayers. © 1997 Elsevier Science B.V.

*Keywords:* Water adsorption; Phloretin; X-ray diffraction; Phospholipid

## 1. Introduction

Phloretin (Ph), which is often used in various membrane studies, reduces the dipole potential within neutral phospholipid bilayers and monolayers [1,2]. Investigators have concluded that changes in the lipid bilayer electrical conductance, resulting from the presence of phloretin in the bilayer, are due to a decrease in the positive dipole potential of the membrane resulting from Ph orienting in the membrane and inserting a dipole potential of opposite polarity to the preexisting potential [3]. Other workers argue, however, that the ability of a compound, such as Ph, to decrease the dipole potential is not a simple function of its dipole moment but depends also on other factors such as the type of substituent on the benzene ring and in the carbon chain [4].

The adsorption of water by lipid bilayers is of great interest and is thought by some investigators to depend on the bilayer dipole potential [5]. In this regard, it has recently been reported that in simple phospholipid systems, Ph decreases the water adsorbed by the lipids [6]; certain Ph analogs were found to have the same effect although these analogs were found to be less potent than was Ph and a possible relationship between the potency of the com-

* Corresponding author. Fax: +1-919-8162812; E-mail: gljendrasiak@rocmac.med.ecu.edu


*PII* S0005-2736(97)00105-3

pounds and their dipole potentials can be inferred from these results. The method of measuring water adsorption in these studies utilized NMR techniques and was, therefore, an indirect measurement; the water adsorption was, moreover, measured at only one partial vapor pressure of water.

In the work presented here, we have obtained water adsorption isotherms for supported multilayers of egg phosphatidylcholine (EPC) singly and together with either 3-(4-hydroxyphenyl)-1-(2,4,6-trihydroxyphenyl)-1-propanone (Ph) or 4′-hydroxyvalerophenone (Hp), a Ph analog. These studies, thus, result in direct measurements of the water adsorbed and, moreover, provide adsorption information over a wide range of partial vapor pressures of water. The water adsorption results are analyzed by BET theory[7] so as to obtain quantitative information on the effects of Ph on the lipid–water interaction. The X-ray diffraction patterns for these EPC–Ph systems, obtained under the same environmental conditions, provide complementary information on the effects of Ph on the lipid bilayer structure and the fluid spacing between adjacent bilayers.

## 2. Materials and methods

The lipids examined in this work were obtained from Avanti Polar Lipids, Alabaster, AL. The lipids were of greater than 99% purity and no additional purification was used. Until the samples were deposited on the Teflon substrates, storage was under prepurified nitrogen at −70°C. The Ph was obtained from Sigma Chemical Co., St. Louis, MO, while the Hp was from Aldrich Chemical Co., Milwaukee, WI.

The experimental technique of using a microbalance as a gravimetric means of measuring physical water adsorption characteristics has been previously reported [8]. A Cahn G-2 electrobalance in the 'remote weighing' mode provided a resolution in the order of $10^{-6}$ g. The temperature during the adsorption process was held at $22.0 \pm 0.2$°C as indicated by an Omega 670 digital thermocouple thermometer with a type T probe.

After a sample was deposited on a substrate it was normally placed within an aluminum chamber and dried under vacuum. It was then moved to the weighing chamber, placed on the balance stirrup and dried under prepurified nitrogen flow until its weight ceased to change. In some cases the samples were placed directly in the weighing chamber under nitrogen flow, again until the weight ceased to change. This constant weight value is defined as the sample's 'dry weight'. Most sample dry weights were 2 to 4 mg. The sample weights used do not significantly affect the results.

Controlled hydration was accomplished by enclosing vessels of saturated salt solutions in the chamber and then purging the system with prepurified nitrogen. The chamber was allowed to reach equilibrium (approximately 24 h) for each hydration determination. More experimental details are available in our previous work [8].

The apparatus included a second sample of the phospholipid deposited on a one by one-sixteenth inch quartz disk. This sample was positioned between and in contact with two $5 \times 5$ mm vacuum deposited electrodes separated by 5 mm. Application of a 2 V direct current source to the sample from the internal power supply of a Keithley 617 programmable electrometer provided concurrent electrical current measurements which were later converted to conductivity values. This electrical technique proved to be a most sensitive indicator of the hydration state of the sample at the lower hydration values.

The fundamental assumption of BET theory is that the same forces that are active in condensation are also those producing the adsorption of the gas on the adsorbent surface. With this assumption, the adsorption isotherm equation is obtained:

$$\frac{p}{v(p_0 - p)} = \frac{1}{v_m c} + \frac{(c-1)}{v_m c} \cdot \frac{p}{p_0} \qquad (1)$$

This is a linear equation and if the theory is obeyed a plot of $p/v(p_0 - p)$ versus $p/p_0$ gives a straight line, where the intercept is $1/(v_m c)$ and the slope is $(c-1)/(v_m c)$. The values for $v_m$ and $c$ can thus be obtained from the experimental data. Here $v$ is the volume of gas adsorbed at the vapor pressure $p$; $v_m$ is the volume of gas adsorbed in a complete unimolecular layer of the gas molecules. The pressure of the gas at saturation is $p_0$ and $c = \exp(E_1 - E_L)/RT$ where $E_1$ is the average heat of adsorption of the gas in the first adsorbed layer and $E_L$ is the heat of liquefaction. Further details of this approach can be found in the elegant work of BET theory [7].

The X-ray diffraction experiments were performed as described in detail previously [9,10]. In brief, EPC and Ph were codissolved in 9:1 (v:v) $CHCl_3$:MeOH at a concentration of approximately 10 mg/ml. A small drop of this solution was placed on a curved glass substrate and the solvent was dried under a gentle stream of nitrogen. The curved glass was mounted in a controlled humidity chamber on a line-focus X-ray camera so that the X-ray beam was oriented parallel to the edge of the glass substrate. The humidity chamber consisted of a copper canister with Mylar windows for passage of the X-ray beam. Relative humidity was controlled in the chamber with a cup of saturated salt solution. To speed equilibrium, a gentle stream of nitrogen was passed through a flask of the saturated salt solution and then through the chamber. The X-ray patterns were recorded on a stack of 6 sheets of Kodak DEF X-ray film in a flat plate cassette. Films were densitometered with a Joyce–Loebl microdensitometer and integrated intensities were obtained for each diffraction order $h$ by measuring the area of the diffraction peak. Structure amplitudes $F(h)$ were obtained from the measured intensities by applying standard correction factors [9,11,12]. Electron density profiles, $\rho(x)$, on a relative electron density scale were calculated from

$$\rho(x) = (2/d)\Sigma\exp\{i\Phi(h)\} \cdot F(h) \cdot \cos(2\pi xh/d) \quad (2)$$

where $x$ is the distance from the center of the bilayer, $d$ is the lamellar repeat period, $\Phi(h)$ is the phase angle for order $h$ and the sum is over $h$. Electron density profiles described in this paper are at a resolution of $d/2h_{max} \approx 7$ Å.

## 3. Results

Fig. 1 shows water adsorption isotherms for EPC alone and in two combinations [1] with Ph. The EPC exhibits a somewhat lower water adsorption below $p/p_0$ values of 0.20 compared to the mixtures. At the higher $p/p_0$ values ($> 0.80$), EPC adsorbs significantly more water than do the other two mixtures. The EPC-Ph isotherms are obtained by calculating the molar ratio of the total water adsorbed to the total EPC present; the Ph, itself, does not exhibit significant water adsorption. Fig. 1 thus illustrates dependence of the water adsorption on the Ph concentration. The adsorption isotherm for EPC–Hp, 3:2 is not shown here but is, within experimental error, congruent with that for EPC–Ph, 4:1.

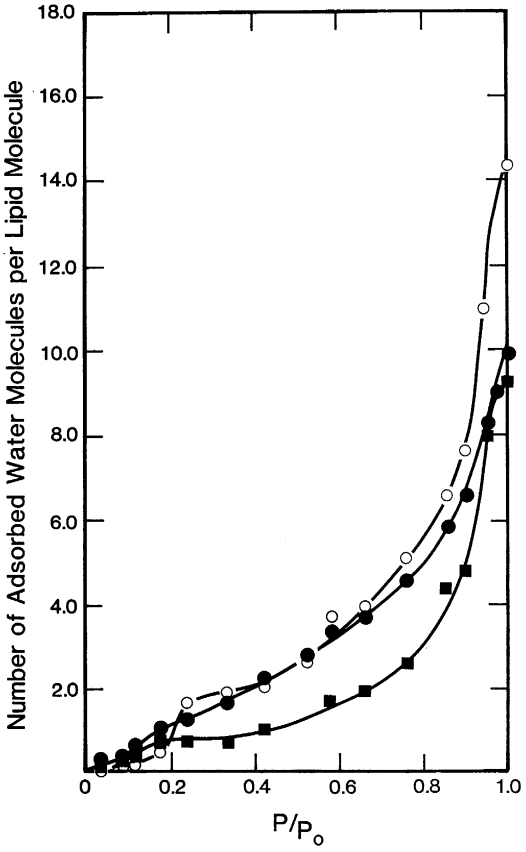


Fig. 1. Adsorption isotherms for EPC (– ○ –), EPC-Ph (4:1, M:M) (– ● –) and EPC-Ph (3:2, M:M) (– ■ –). Ph itself adsorbs a very small amount of water. The isotherms are calculated as if all of the EPC was adsorbing water independently of the presence of Ph.

In Fig. 2 are shown BET plots calculated from adsorption isotherms shown in Fig. 1. Note the large deviation from linearity, for the EPC plot at $p/p_0$ values $< 0.20$ vis-á-vis the BET plot for EPC–Ph, 3:2. The BET plots for EPC–Ph, 4:1, and EPC–Hp, 3:2, not shown, also maintain their straight line character at $p/p_0$ values $< 0.20$. The deviation from a

[1] All ratios of EPC with other materials are expressed as mol:mol (M:M).

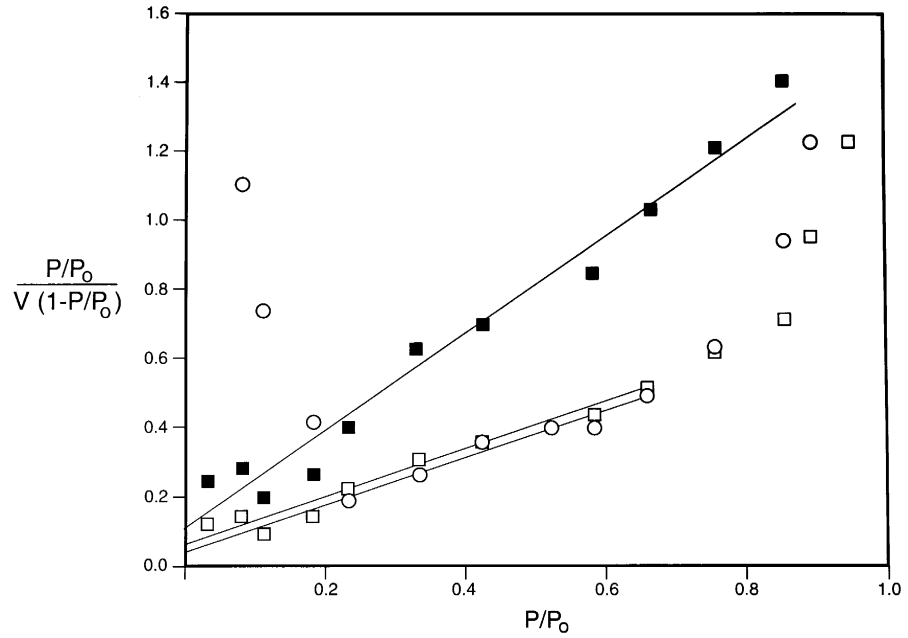


Fig. 2. BET plots for EPC (– ○ –), EPC–Ph (3:2, M:M) (– ■ –) and EPC–Ph (3:2, M:M) (– □ –). Note that the BET plot for EPC:Ph designated by (– ■ –) is calculated from Fig. 1, i.e. assuming all of the EPC present adsorbs water as it does when present alone. The EPC:Ph BET plot designated by (– □ –) is calculated as if 0.5 of the EPC adsorbs water as if no Ph was present. See text for further details.

straight line at the higher humidities is shown for all lipids studied and other materials as well. Note that here the BET plots for EPC–Ph, 3:2 are displayed in two ways: (1) assuming all of the EPC present in the mixture adsorbs water as if no Ph were present and (2) assuming one-half of the EPC present adsorbs water as if no Ph were present whereas the other one-half adsorbs essentially no water. More will be said about this latter method of calculation below.

In Table 1 are listed the results obtained from applying Eq. (1) to the BET plots which are, in turn, calculated from the respective water adsorption isotherms. The BET parameter $v_m$ is associated with the number of water molecules in the first 'monolayer' of water adsorbed by the adsorbing surface and $E_1$ is the binding energy of this monolayer to this surface [7]. The number of samples for which isotherms have been obtained is given by $n$. The

Table 1
BET constants and assumptions

| Phospholipids and mixtures | $n$ | $p/p_0$ (range) | $v_m$ (molecules water per lipid molecule) | $E_1$ (kcal/mol) | $r$ |
|---|---|---|---|---|---|
| EPC | 7 | 0.23–0.66 | 1.41 | 11.4 | 0.97 |
| EPC–Ph (3:2, M:M) (all EPC available) | 4 | 0.03–0.86 | 0.66 | 11.2 | 0.99 |
| EPC–Ph (3:2, M:M) (0.67 EPC available) | 4 | 0.03–0.76 | 1.02 | 11.0 | 0.99 |
| EPC–Ph (3:2, M:M) (0.50 EPC available) | 4 | 0.03–0.66 | 1.40 | 11.0 | 0.98 |
| EPC–Ph (3:2, M:M) (0.33 EPC available) | 4 | 0.03–0.76 | 2.15 | 11.8 | 0.99 |
| EPC–Ph (4:1, M:M) (all EPC available) | 2 | 0.03–0.58 | 1.67 | 10.6 | 0.95 |
| EPC–Ph (4:1, M:M) (0.75 EPC available) | 2 | 0.03–0.58 | 2.22 | 10.6 | 0.95 |
| EPC–Hp (3:2, M:M) (all EPC available) | 2 | 0.03–0.58 | 1.65 | 10.6 | 0.97 |
| EPC–Hp (3:2, M:M) (0.67 EPC available) | 2 | 0.03–0.58 | 2.51 | 10.6 | 0.97 |

correlation coefficients shown in the last column are given for the straight line portion of the BET plots.

In the first column of Table 1, in the parentheses, are shown the assumptions used for calculating the BET parameters shown in the respective rows. For example, in the first row, all EPC is assumed available for water adsorption since no other material is present (see Fig. 2). In the fourth row, however, we assume that one-half (0.5) of the EPC, on average, adsorbs water as it would if present alone whereas the remaining one-half of the EPC adsorbs water as if the adsorption process is affected by the presence of the Ph (see Fig. 2); this approach is reasonable since the weight of the water adsorbed by the EPC with the Ph present is less than the weight of the water adsorbed by the same amount of EPC but with no Ph present. Since the $v_m$ (and $E_1$) values obtained using this assumption are very close to those obtained for EPC alone, this assumption is designated the 'most reasonable case'. The other values for $v_m$ and $E_1$ given in the table are calculated in a similar manner but with the respective assumptions given in the first column. The $v_m$ values were calculated for the EPC–Ph, 4:1 and the EPC–Hp cases, by using the BET equation and assuming that all of the EPC is free to adsorb water as if EPC were present alone (rows 6 and 8). Although, these $v_m$ values are not as close to the $v_m$ value calculated for EPC when adsorbing by itself (row 1) as is the $v_m$ calculated for EPC–Ph, 3:2, nevertheless, they are as close as obtainable using the BET equation, no matter what assumptions are made.

In Fig. 3 are shown the water adsorption isotherms for EPC and EPC–Ph, 3:2 but in contradistinction to Fig. 1, the isotherm for EPC–Ph is calculated by assuming that one-half (0.5) of the EPC present adsorbs water in a manner similarly to the way it does with no Ph present whereas little, if any, water adsorption is assumed to occur by the remaining EPC. The two isotherms are similar in appearance, however, they are displaced along the $p/p_0$ axis from one another at $p/p_0$ values $< 0.20$; the isotherms at the higher $p/p_0$ values also differ from each other. Note that Fig. 2 shows the BET plots obtained from these isotherms. From these BET plots, the parameters shown in Table 1, fourth row, are calculated.

The X-ray diffraction patterns from EPC, EPC–Ph, 4:1 and EPC–Ph, 3:2 specimens for $0.32 < p/p_0 < 0.98$ gave diffraction patterns containing several sharp low-angle reflections that indexed as orders of a lamellar repeat period. Previously, McIntosh et al. [9] found that for $p/p_0 < 0.32$, EPC gave a second set of lamellar reflections with a much larger repeat period, consistent with the formation of a gel phase. This second set of reflections was not, however, observed for EPC–Ph, 3:2 specimens for $p/p_0$ values of 0.23 and 0.15. Fig. 4 shows the lamellar repeat periods for the EPC, EPC–Ph, 4:1, and EPC–Ph 3:2 specimens for $0.32 < p/p_0 < 0.98$. At a given humidity, the repeat period decreased with increasing Ph concentration, and at a given Ph concentration the

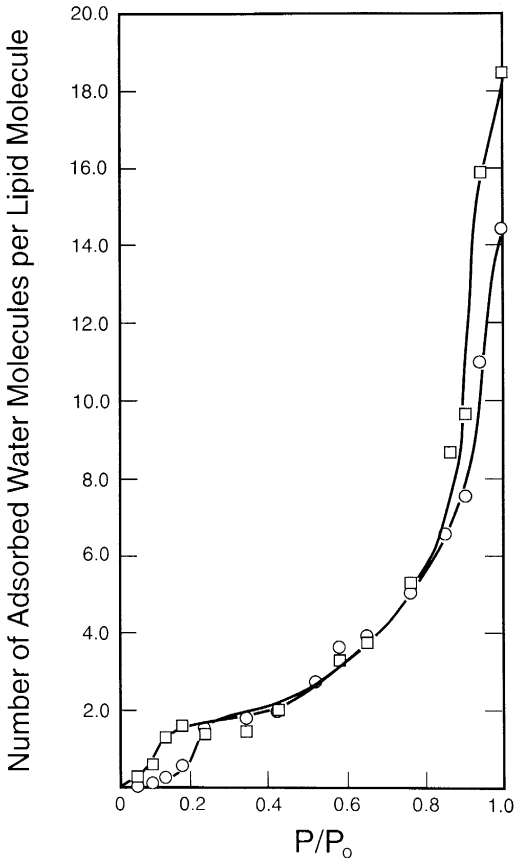


Fig. 3. Water adsorption isotherms for EPC (– ○ –) and EPC–Ph (– □ –) (3:2, M:M). The isotherm for EPC–Ph is calculated by assuming that 0.5 of the EPC present adsorbs water as it would if present alone; the adsorption of the remaining 0.5 EPC is assumed to be altered by the presence of Ph. These plots should be compared with those shown in Fig. 1.

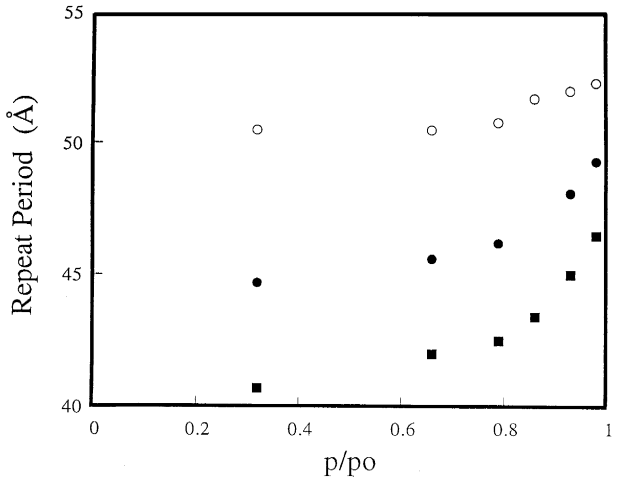


Fig. 4. Lamellar repeat period plotted versus $p/p_0$ for EPC (○); EPC–Ph (4:1, M:M) (●) and EPC–Ph (3:2, M:M) (■). EPC data taken from Ref. [9].

repeat period decreased with decreasing relative humidity.

The lamellar repeat period contains contributions from both the bilayer and the intervening fluid layer. To obtain information on the effects of Ph on both the bilayer thickness and the fluid layer thickness a Fourier analysis of the X-ray data was performed. Fig. 5 shows the structure amplitude data plotted versus the reciprocal spacing for EPC, EPC–Ph, 4:1 and EPC–Ph, 3:2. The structure amplitudes for the EPC–Ph specimens were similar, but not identical to the EPC data. Based on this comparison of the structure amplitude data (Fig. 5), we used the equivalent phase angles ($\Phi(h)$) for the EPC–Ph samples as for EPC [9,13].

Fig. 6 shows electron density profiles for EPC and EPC–Ph, 3:2 obtained at $p/p_0 = 0.98$. For each profile, the bilayer center is at the origin. For EPC, the high electron density peaks at $\pm 19$ Å correspond to the polar head groups and the low density region in the middle of the bilayer corresponds to the hydrocarbon core of the bilayer. The low density regions at the outer edges of the profile correspond to the narrow fluid spaces between apposing bilayers. For EPC–Ph, 3:2, the distance between head group peaks across the bilayer is smaller, indicating that the incorporation of Ph has decreased the bilayer thickness, or equivalently increased the area per phospholipid molecule. At $p/p_0 = 0.98$, the distance between head group peaks across the bilayer was 38 Å for EPC, 35 Å for EPC–Ph, 4:1 and 33 Å for EPC–Ph, 3-2.

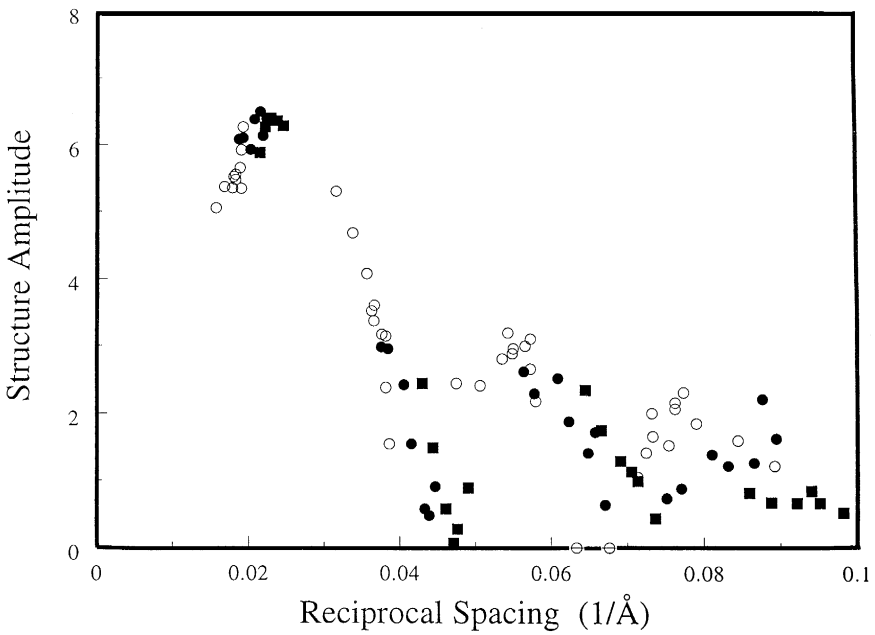


Fig. 5. X-ray diffraction structure amplitudes plotted versus reciprocal space coordinate for EPC (○); EPC–Ph (4:1, M:M) (●) and EPC–Ph (3:2, M:M) (■). EPC data from Ref. [9].

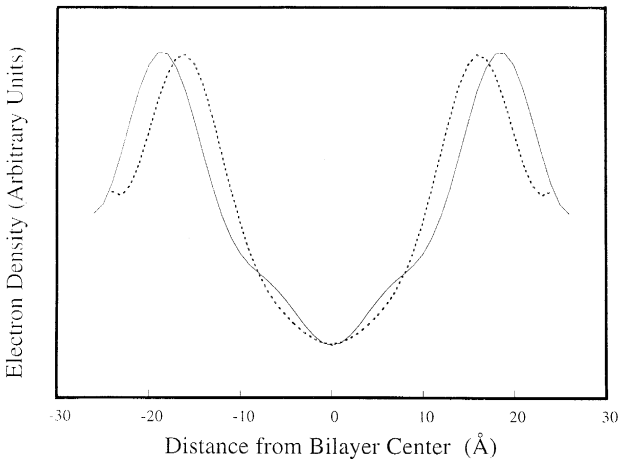


Fig. 6. Electron density profiles for EPC (solid line) and EPC–Ph (3:2, M:M) (dotted line) at $p/p_0 = 0.98$. In each profile one unit cell is shown, with the bilayer center at 0 Å. EPC data taken from Ref. [9].

Fig. 7 shows electron density profiles of EPC–Ph, 3:2 as a function of relative humidity. The shape of the bilayer region of the profiles shows relatively little change with decreasing relative humidity. Evidence for this is that high density peak-to-peak spacing across the bilayer stayed approximately constant (dpp 33.3 ± 0.9 Å) over this range of relative humidity, although the peak-to-peak distance did increase slightly at the lowest relative humidities (Fig. 7). The profiles in Fig. 7 also show that the fluid layers at the outer edges of the profile decreased with decreasing relative humidity.

We use the electron density profiles to estimate the change in interbilayer fluid spacing as a function of relative humidity. As shown elsewhere [9,10,13–16] electron density profiles, such as those in Figs. 6 and 7, can be used to estimate the fluid space between apposing bilayers for each value of applied pressure. The definition of the lipid/water interface is somewhat arbitrary, because the bilayer surface is not smooth and water penetrates into the head group region of the bilayer [17–19]. We operationally define the bilayer width as the total physical thickness of the bilayer assuming that the conformation of the phosphorylcholine head group in bilayers is the same as it is in single crystals of phosphatidylcholine [20]. In that case, the high density head group peak in the electron density profiles would be located between the phosphate group and the glycerol backbone, so that the edge of the bilayer lies about 5 Å outward from the center of the high density peaks in the electron density profiles [9,10,14,16].

Using the above definition for the bilayer/water interface, we plot in Fig. 8 the distance between bilayers as a function of $p/p_0$ for EPC, EPC–Ph, 4:1 and EPC–Ph, 3:2. Two main features of this figure are that: (1) for a given specimen, the distance between bilayers decreases with decreasing relative hu-

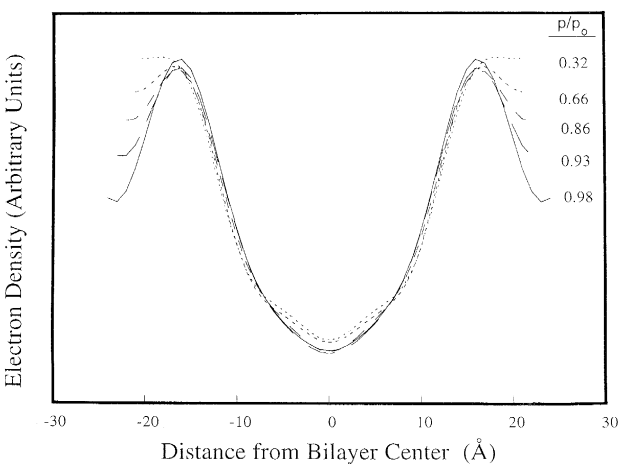


Fig. 7. Electron density profiles for EPC–Ph (3:2, M:M) as a function of relative humidity. In each profile one unit cell is shown, with bilayer center at 0 Å.

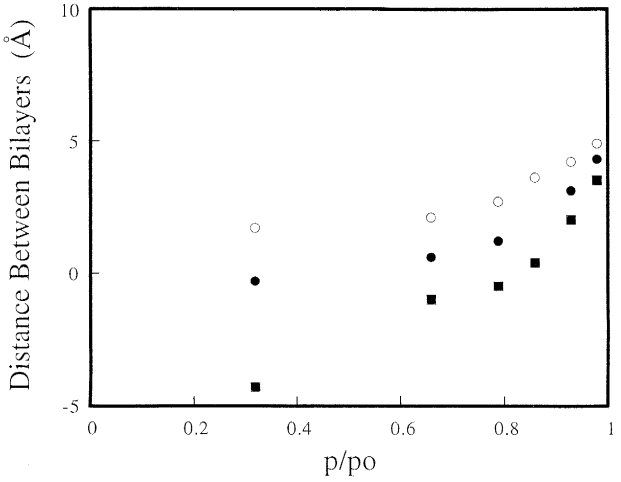


Fig. 8. Distance between adjacent bilayers plotted versus $p/p_0$ for EPC (○); EPC–Ph (4:1, M:M) (●) and EPC–Ph (3:2, M:M) (■).

midity and (2) at a given humidity the distance between bilayers decreases with increasing Ph concentration. In particular, for EPC–Ph, 3:2 at $p/p_0 =$ 0.32, the distance between bilayers was negative, indicating head groups from apposing bilayers interpenetrated, consistent with the electron density profile (Fig. 7) which demonstrated a partial merging of the head group peaks from apposing bilayers.

## 4. Discussion

Our adsorption measurements show that Ph and, to a lesser extent, its analog Hp, when present with EPC, decrease the water adsorbed by EPC multilayers for $p/p_0$ values $> 0.20$; the respective adsorption isotherms, nevertheless, are indicative of 'strong' water binding [7], as is the isotherm for EPC itself. This direct determination of decreased hydration is qualitatively in agreement with that found, using NMR measurements [6], for water adsorption at the single $p/p_0$ value of 0.90. The effect of Hp at a molar ratio of EPC–Hp, 3:2, on water adsorption is about the same as that of Ph at a molar ratio of EPC–Ph, 4:1; our gravimetric results are thus again in agreement with those obtained by deuterium NMR techniques [6], at least for the single $p/p_0$ value of 0.90. Since the NMR results are given only for the $p/p_0$ value of 0.90, a comparison at other $p/p_0$ values cannot be made at this time. The two measurement techniques, i.e. gravimetric and NMR, however, are very different and, furthermore, the preparation of the phospholipid samples also differs between the two experimental approaches. Our results, although consistent with an electric dipole effect on the water adsorption, nevertheless, should not necessarily be taken to substantiate this interpretation, discussed in Ref. [5], since other explanations are possible.

The adsorption studies, depending on the assumptions made, suggest that the water binding of only some of the EPC molecules, when EPC is in excess, can be regarded as affected by the Ph while the remaining EPC molecules can be considered to adsorb water as they do with no Ph present. In Fig. 3, the isotherm for EPC–Ph, 3:2 is replotted assuming that one-half of the EPC molecules adsorb as if the Ph had little, if any, effect on the adsorption; the isotherm then closely resembles that for EPC, alone except for the displacement along the $p/p_0$ axis. The $v_m$ in row 4, Table 1, which is calculated for the one-half of the EPC molecules assumed not to interact with the Ph molecules, has the same $v_m$ value as that calculated for EPC with no Ph present and, because of this agreement, we refer to this assumption as the 'most reasonable case'. A similar line of reasoning is followed for both EPC–Ph, 4:1 and EPC–Hp, 3:2, where all of the EPC is assumed to be available for water adsorption. The $v_m$ values calculated in these latter two cases are greater than that found for EPC alone, but nevertheless, these $v_m$ values are still closer to that obtained for EPC than those obtained with any other interaction assumptions. It may well be that, due to the lower amount of Ph and the weaker effect of Hp, the sensitivity of our measurements is insufficient to more accurately measure the small effects on the EPC adsorption.

Additionally, no matter what assumptions are made, the $E_1$ values obtained using BET theory [7], for the binding energies of the first monolayer of water adsorbed, are close to the value for the energy of two hydrogen bonds [21]. These $E_1$ values are also similar to those calculated by us for other lipid systems [8]. This would suggest an 'ice-like' state for this first monolayer of water adsorbed and is further supported by our electrical conductivity measurements (work in progress).

The BET plot for EPC (Fig. 2) obtained from the isotherm in Fig. 1 deviates rather strongly from a straight line at $p/p_0$ values $< 0.23$, i.e. the $p/p_0$ value where EPC absorbs between one and two water molecules per EPC molecule. This deviation results from the fact that the water adsorption isotherm for EPC (Fig. 1) displays a rapid decrease in adsorption that occurs when $p/p_0 < 0.20$; on the basis of the surface studies discussed in Ref. [7], however, one would expect this sharp drop in water adsorption to begin at $p/p_0$ values nearer zero. These results, thus, suggest a structural change in the EPC multilayer when $p/p_0 < 0.20$ and the BET parameters (Table 1) for EPC alone, likely apply to this 'structurally altered' EPC film. The X-ray data for EPC do indeed show a structural change from a gel phase to the liquid crystalline phase as evidenced by a sharp increase in the lamellar repeat period[9] at $p/p_0$ values of 0.15 and 0.20. No such increase in repeat period, nor change in phase, is observed with EPC–

Ph, 3:2 for $p/p_0$ values of 0.15 to 0.23. The presence of the Ph with the EPC, moreover, results in both a straight line BET plot extending to the dry state value, i.e. $p/p_0 = 0$ (Fig. 2) and an altered water adsorption isotherm (Fig. 1) which does not exhibit the sharp hydration decrease near $p/p_0 = 0.20$ that EPC does when present by itself. As discussed in Ref. [6], Ph has three hydroxyl groups in the same ring system which could be involved in hydrogen bonding to the lipid head group; this, in turn, could result in the removal of the EPC phase change. The result of this removal would be the initial rapid rise in hydration of the phospholipid below $p/p_0 = 0.20$ shown in Fig. 1 and the resultant straight line BET plot shown in Fig. 2. The X-ray diffraction data show that liquid crystalline lipid bilayers are present for EPC, for values of $p/p_0$ from 0.32 to 0.98 and for $p/p_0$ values from 0.15 to 0.98 for EPC–Ph, 4:1 and EPC–Ph,3:2. Interestingly, Ph when present in EPC–Ph, 3:2, removes the transition at $p/p_0$ values $<$ 0.20, shown by EPC alone, and decreases the total water adsorbed at the higher $p/p_0$ values. Ph when present in EPC–Ph, 4:1 and Hp when present in EPC–Hp 3:2 do not show a large effect on the water adsorption at the higher humidities (0.20–0.90) nevertheless, they do produce a very similar removal of the phase transition at the lower humidities ( $p/p_0 <$ 0.20). The concentration dependence for Ph in removing the EPC phase transition thus differs from that involved in decreasing the total water adsorption by EPC. The introduction of Ph decreases the bilayer thickness, indicating an increase in area per lipid molecule, consistent with Ph being located in the interfacial region of the bilayer and, therefore, increasing the lateral distance between EPC molecules. Previously [13], we have found that the area per molecule of EPC is about 64 Å$^2$. Since the width of the EPC head group[13] is about 10 Å, we estimate from the electron density profiles that the width of the hydrocarbon region of the bilayer is 28 Å for EPC, 25 Å for EPC–Ph, 4:1 and 23 Å for EPC–Ph, 3:2. Assuming that the volume of the hydrocarbon chain region remains constant with the incorporation of Ph, then we estimate that the area per EPC molecule is about 72 Å$^2$ for EPC–Ph, 4:1 and about 78 Å$^2$ for EPC–Ph, 3:2.

The introduction of Ph also causes a large decrease in the fluid space between adjacent bilayers (Fig. 8). An explanation for this decrease in fluid layer thickness is a phloretin-induced reduction in the short-range repulsive pressures between apposing bilayers. The repulsive hydration pressure would be expected to be reduced by the presence of Ph, since Ph reduces the dipole potential, which has been related to the magnitude of the hydration pressure [5]. Moreover, short-range steric repulsion [9] between apposing bilayers should also be reduced by the incorporation of Ph, since Ph increases the area per EPC head group and the steric pressure decreases with increasing area per EPC head group [10].

Therefore, the structural data indicate that the volume available for water in these multilayers, which can be related to the adsorption isotherms, is modified in two ways by the incorporation of phloretin–the area per EPC molecule is increased and the width of the fluid space is decreased. The increase in area per EPC molecule would tend to increase the volume available for water, whereas the decrease in fluid separation would tend to decrease the water volume. However, the percentage decrease in fluid separation is larger than the percentage increase in area per EPC molecule, indicating that the incorporation of Ph decreases the volume of water in the multilayers. Thus, the structural results are consistent with the adsorption results which show a decreasing water content with increasing Ph concentration (Fig. 1).

It should be mentioned here that Ph, because of its OH groups bears some structural similarity to trehalose. The role of trehalose in cryobiology and its relationship to bound water is actively under investigation. It has been proposed in the ‘water replacement hypothesis’ [22,23] that the depression of the phase transition temperature, observed in phospholipids, involves a direct interaction between the sugar and phospholipid head groups. Other workers, however, conclude that the transition temperature of certain fully hydrated phospholipids is hardly influenced by the addition of trehalose [24]. Our results indicate that both Ph and Hp do remove the phase transition observed in dry EPC multilayers by increasing the EPC adsorbed water at the very low water partial pressures. This could well arise because of the increased head group area caused by the presence of Ph (or Hp). Although we are presently investigating the role of sugar and glycolipids in influencing the water adsorption characteristics of phospholipids (work in

progress), nevertheless, this matter is a rather complex one. At this point we can say that Ph (and its analog) certainly influences the water adsorption characteristics of EPC, increases the area of the EPC molecule and decreases the width of the fluid space between the bilayers.

## Acknowledgements

This work was supported in part by NIH Grant GM-27278 and a grant from the Southern Regional Education Board. Special thanks go to Ms. Melissa Card for her cooperation and patience in typing this manuscript. Parts of this work were presented at the 40th Annual Meeting of the Biophysical Society, 1996 (Biophys. J. 70, p. 89).

## References

[1] E. Melnik, R. Latorre, J.E. Hall, D.C. Tosteson, J. Gen. Physiol. 69 (1977) 243–257.
[2] W.R. Perkins, D.S. Cafiso, J. Membr. Biol. 96 (1987) 165–173.
[3] O.S. Andersen, A. Finkelstein, A. Cass, J. Gen. Physiol. 67 (1976) 749–771.
[4] J. Reyes, F. Greco, R. Motais, R. Latorre, J. Membr. Biol. 72 (1983) 93–103.
[5] S.A. Simon, T.J. McIntosh, Proc. Natl. Acad. Sci. USA 86 (1989) 9263–9267.
[6] B. Bechinger, J. Seelig, Biochemistry 30 (1991) 3923–3929.
[7] S. Brunauer, The Adsorption of Gases and Vapors, vol. 1, Princeton University Press, Princeton, 1943.
[8] G.L. Jendrasiak, R.L. Smith, W. Shaw, Biochim. Biophys. Acta 1279 (1996) 63–69.
[9] T.J. McIntosh, A.D. Magid, S.A. Simon, Biochemistry 26 (1987) 7325–7332.
[10] T.J. McIntosh, A.D. Magid, S.A. Simon, Biochemistry 28 (1989) 17–25.
[11] A.E. Blaurock, C.R. Worthington, Biophys. J. 6 (1966) 305–312.
[12] L. Herbette, J. Marquardt, A. Scarpa, J.K. Blasie, Biophys. J. 20 (1977) 245–272.
[13] T.J. McIntosh, A.D. Magid, S.A. Simon, Biochemistry 28 (1989) 7904–7912.
[14] T.J. McIntosh, S.A. Simon, Biochemistry 25 (1986) 4058–4066.
[15] T.J. McIntosh, S.A. Simon, Biochemistry 32 (1993) 8374–8384.
[16] T.J. McIntosh, S.A. Simon, D. Needham, C.H. Huang, Biochemistry 31 (1992) 2020–2024.
[17] O.H. Giffith, P.J. Dehlinger, S.P. Van, J. Membr. Biol. 15 (1974) 159–192.
[18] S.A. Simon, T.J. McIntosh, R. Latorre, Science 216 (1982) 65–67.
[19] D.L. Worcester, N.P. Franks, J. Mol. Biol. 100 (1976) 359–378.
[20] R.H. Pearson, I. Pascher, Nature 281 (1979) 499–501.
[21] F.M. Snell, S. Shulman, R.P. Spencer, C. Moos, Biophysical Principles of Structure and Function, Reading, 1965, p. 49.
[22] J.H. Crowe, L.M. Crowe, D. Chapman, Science 223 (1984) 701–703.
[23] J.H. Crowe, F.A. Hoekstra, K.H.N. Nguyen, L.M. Crowe, Biochim. Biophys. Acta 1280 (1996) 187–196.
[24] M. Nakagaki, H. Nagase, H. Ueda, J. Membr. Sci. 3 (1992) 173–180.